Kinetic Studies on the Removal of Iron and Aluminum from Recombinant and Site-Directed Mutant N-Lobe Half Transferrins†

Yuejin Li,‡ Wesley R. Harris,*,‡ Alexis Maxwell,§ Ross T. A. MacGillivray,§ and Todd Brown‡

Department of Chemistry, University of Missouri−St. Louis, St. Louis, Missouri 63121,and Department of Biochemistry, University of British Columbia, Vancouver, British Columbia V6T 1Z3

Received May 6, 1998; Revised Manuscript Received August 7, 1998

ABSTRACT: Kinetic studies have been conducted in pH 7.4 Hepes buffer at 25 °C on the removal of Fe(III) and Al(III) from the recombinant N-lobe half molecule of human serum transferrin (Tf/2N) and from the R124A, K206A, and K296A mutants of this protein. The rates of iron removal from Tf/2N by 3-hydroxypyridin-4-one (deferiprone) and nitrilotriacetic acid (NTA) are essentially identical with previous results on N-terminal monoferric transferrin (Tf-Fe_N). For both Tf/2N and Tf-Fe_N, iron removal by deferiprone follows simple saturation kinetics, while iron removal by NTA follows simple first-order kinetics. There is some discrepancy between the two proteins with respect to iron removal by PP_i, but this may be due to differences in the chloride concentrations among different studies. The addition of $Fe(NTA)_2$ to R124A at ambient bicarbonate concentrations forms the Fe−NTA−Tf ternary complex, but the usual Fe−CO_3−Tf complex can be formed by adding ferrous ion in the presence of a larger excess of bicarbonate. This complex releases its iron very rapidly by a mechanism that is first-order with respect to the ligand. This suggests that the first-order component of metal release from transferrin involves the displacement of the synergistic carbonate anion. Since iron removal from K206A and K296A at pH 7.4 is extremely slow, studies have been conducted on the more labile Al^{3+} complexes of Tf/2N, K206A, and K296A. The removal of Al^{3+} from Tf/2N by PP_i follows the same complex kinetic order with respect to the ligand concentration that is observed for iron removal, while the removal of Al^{3+} from both K206A and K296A reverts to a simple saturation process. The addition of perchlorate retards the removal of Al^{3+} from both K206A and K296A, suggesting that these lysine residues are not associated with the allosteric effects of inorganic anions on the rates of metal removal.

Serum transferrin is the protein which binds iron as Fe^{3+} and transports this otherwise insoluble cation through the blood (*1*−*5*). Transferrin belongs to a small family of iron-binding proteins that includes lactoferrin and ovotransferrin. These proteins were originally distinguished by the essential role of carbonate in the metal-binding process. One carbonate anion is tightly bound along with each ferric ion, and essentially no metal binding is observed in the absence of carbonate.

Several crystal structures of serum transferrin and other transferrins have been reported (*6*−*16*). Although the protein consists of a single polypeptide chain, it folds into two distinct, structurally similar lobes that are connected by a short polypeptide segment. Each lobe contains a single, high-affinity iron-binding site. The protein provides four ligating groups to each iron. These groups consist of the side chains of one histidine, two tyrosines, and one aspartic acid residue. The carbonate acts as a bidentate ligand and occupies the fifth and sixth coordination sites on the iron (*8*, *10*). This same set of ligating groups is found in both the C-terminal- and N-terminal-binding sites of transferrin, lactoferrin, and ovotransferrin, with only rather minor differences in coordination geometry among the three proteins. The carbonate, which is referred to as the synergistic anion, is also bound by noncovalent interactions to the guanidinium side chain of an arginine residue, the hydroxyl group of a threonine side chain, and to main-chain amide groups at the terminus of an α-helix.

The mechanism by which iron is released from transferrin to low molecular weight chelating agents has been investigated extensively, but it is still not well understood. Several systems have shown saturation kinetics with respect to the free ligand concentration (*17*−*22*), while iron removal by NTA[1] and DTPA follows simple first-order kinetics (*23*, *24*), and several other ligands appear to follow a combination of both saturation and first-order components (*18*, *23*−*30*).

† This work was supported by Grant DK35533 from the National Institutes of Health.

* Address correspondence to this author. Fax: 314-516-5342. E-mail: wharris@umsl.edu.

‡ University of Missouri−St. Louis.

§ University of British Columbia.

[1] Abbreviations: Hepes, *N*-(2-Hydroxyethyl)piperazine-*N*′-(2-ethanesulfonic acid); Tf-Fe_N, transferrin with iron loaded selectively into the N-terminal-binding site; Tf/2N, recombinant N-lobe of human serum transferrin, consisting of residues 1−337; PP_i, pyrophosphate; deferiprone, 1,2-dimethyl-3-hydroxypyridin-4-one; NTA, nitrilotriacetic acid; EDTA, ethylenediaminetetraacetic acid; DTPA, diethylenetriaminepentaacetic acid; AHA, acetohydroxamic acid; tiron, 1,2,-dihydroxybenzene-3,5-disulfonic acid.

S0006-2960(98)01045-9 CCC: $15.00
Published on Web 09/17/1998

There is general agreement that the iron removal process is controlled, at least in part, by a gating conformational change in the protein. Crystallographic studies have confirmed that there is a major conformational change between the ferric- and apotransferrin structures (*6*, *15*), but the precise nature of the rate-limiting step in iron release is still not known.

The kinetics of iron release have shown a very complicated dependence on the concentration of anions in the solution (*18*, *29*−*36*). This suggests the presence of an allosteric binding site, which is often referred to as the kinetically significant anion binding (KISAB) site to distinguish it from the binding site of the synergistic carbonate anion. There are two lysine side chains (Lys 206 and Lys 296 in Tf/2N) near the iron that could be involved in the KISAB site (*4*, *5*, *37*, *38*). To assess the role of each charged residue in the iron release process, we have begun a study on iron release from a series of recombinant transferrins in which these cationic residues are replaced by neutral alanine side chains. To simplify the kinetics and to facilitate the production of relatively large amounts of recombinant proteins, these studies have been conducted on the isolated N-lobe of transferrin.

In this paper, we report on iron and aluminum release from the recombinant N-lobe half molecule of human serum transferrin (Tf/2N) and from the N-lobe mutants R124A, K206A, and K296A. Arginine 124 is one of the residues involved in binding the synergistic bicarbonate anion. Lysines 206 and 296 are near the metal-binding site but are not directly involved in iron binding. In the course of this study, we found that iron release from the mutants K206A and K296A is so slow that it is essentially impossible to characterize the ligand dependence of the reaction. Therefore, the study was expanded to include kinetic studies using the more labile Al^{3+}−protein complexes as functional models of the corresponding ferric complexes.

MATERIALS AND METHODS

Materials. All solutions were prepared with distilled water, which was further purified by passage through a Millipore MilliQ water system. Acetohydroxamic acid (AHA) and sodium pyrophosphate were purchased from the Aldrich Chemical Co. and Sigma Chemical Co., respectively. To generate a neutral solution of PP_i without other anions, a stock solution of pyrophosphoric acid was first prepared by passing $Na_4P_2O_7$ through Dowex 50W-X8 (H-type) cation-exchange resin. The pH of the solution was then adjusted to 7.4 by the addition of NaOH. Deferiprone was synthesized according to reported procedures (*39*).

The stock solution of ferric chloride was standardized by passage through Dowex 50W-X8 cation-exchange resin. The eluted acid was titrated with standard KOH solution, which was prepared from CO_2-free commercial concentrate (Baker Dilut-it ampules). Bis(nitrilotriacetato)ferrate(III) was prepared by dissolving nitrilotriacetic acid (NTA) in water, adding the appropriate volume of a pH 1 solution of ferric chloride, and slowly raising the pH to 4.0 by the dropwise addition of NaOH. Solutions of ferrous ammonium sulfate were prepared fresh daily in septum bottles using water that had been rendered O_2-free by bubbling with argon. The pH of the ferrous solutions was maintained at pH 4.5.

Hepes was used as the buffer in all experiments. The pH of buffer solutions was measured using a Fisher Accumet model 25 pH meter fitted with a Fisher combination electrode. The pH meter was calibrated before use with two standard buffer solutions (Fisher). All solutions of proteins and iron removal reagents were adjusted to pH 7.4 with NaOH.

T4 ligase and restriction endonucleases were purchased from Pharmacia and Gibco/BRL. [^{35}S]dATP was purchased from NEN−Dupont. All DNA sequence analyses were performed using Sequenase version 2.0 from Amersham/USB. *Taq* polymerase was purchased from Perkin-Elmer Cetus. Baby hamster kidney (BHK) cells were maintained on Dulbecco's modified Eagle's Medium-Ham-F-12 nutrient mixture with phenol red (Gibco/BRL) supplemented with 5% newborn calf serum (catalog no. 200-6010AJ Gibco/BRL). The serum replacement UltroSer G was also purchased from Gibco/BRL. Methotrexate (from David Bull Laboratories) was purchased from the local hospital pharmacy. Corning-brand expanded surface roller bottles (2000 mL capacity), as well as 50 and 250 mL canted neck tissue culture flasks, were obtained from a local distributor. PM 10 diaflo ultrafiltration membranes and a CH2 concentrator fitted with an S1Y10 spiral cartridge were purchased from Amicon. For use in ELISAs, the antibody αHTFN+N1 (specific to the N-lobe of human transferrin), a steptavidin−HRP conjugate, and biotinylated antigen were obtained from Dr. Anne B. Mason (Department of Biochemistry, The University of Vermont); the secondary antibody was purchased from UNLB and Affinity Biologicals Inc. The transferrin used for the standard curve was from Sigma.

In Vitro Mutagenesis. All DNA manipulations were performed using the human transferrin N-lobe cDNA clone that has been described previously (*40*). Plasmid DNA was purified from *Escherichia coli* DH5αF′ cells. The cDNA was cloned into the Bluscript KS^+ plasmid and was engineered to contain *Not*I sites at both ends of the cDNA to facilitate its cloning into a modified pNUT expression plasmid (*41*).

Fragments of the TF/2N cDNA were subcloned to provide templates for polymerase chain reaction-directed mutagenesis (*42*). For mutagenesis of the Arg 124 codon, a 247 bp *Bam*HI−*Hin*cII fragment [nucleotides 354−601 using the numbering of Yang et al. (*43*)] was subcloned into the *Bam*HI and *Hin*cII sites of Blue Script SK^+. For mutagenesis of the Lys 206 and Lys 296 codons, a 469 bp *Hin*cII−*Hin*dIII fragment (nucleotides 928−1070) was subcloned into the *Hin*cII and *Hin*dIII sites of Bluescript KS^+. Together with Bluescript-specific flanking primers, the following mutagenic oligonucleotides were used as primers to introduce the desired mutations:

R124A: 5′-CTAGGC<u>GCC</u>TCCGCTGGGTGGAAC-3′

R124E: 5′-CTAGGC<u>GAG</u>TCCGCTGGGTGGAAC-3′

K206A: 5′-TGGCCTTTGTC<u>GCC</u>CACTCGA-3′

K296A: 5′-CCTGCTGTTT<u>GCC</u>GACTCTGCCCA-3′

In each case, the mutated codon is underlined. Mutagenesis was carried out as described by Nelson and Long (*42*) using the following conditions: denaturation was at 94 °C

for 15 s, annealing was at 50 °C for 30 s, and extension was at 72 °C for 30 s. Step I of the PCR-mutagenesis procedure consisted of 30 cycles, step II consisted of 2 cycles, and step III consisted of 30 cycles.

After mutagenesis, the individual DNA fragments were purified by agarose gel electrophoresis, isolated by electroelution, cleaved with *Hin*cII and *Bam*HI or *Hin*cII and *Hin*dIII, and subcloned back into the corresponding sites of either Blue Script KS^+ or SK^- plasmids. The complete nucleotide sequence of each mutated fragment was then determined to confirm the presence of the mutation and to confirm the absence of other mutations introduced during the PCR steps. The fragments were then cloned back into the TF/2N cDNA clone; restriction endonuclease mapping and DNA sequence analysis were used to confirm the orientation and flanking sequences of the final constructs. The TF/2N cDNAs were then ligated into a *Not*I site that had been engineered in place of the *Sma*I sites of the expression vector pNUT (*41*). The correct orientation of the cDNA in pNUT was confirmed by restriction endonuclease mapping and DNA sequence analysis.

Transfection of Baby Hamster Kidney Cells. BHK cells were transfected with 20 μg of the purified plasmids using the calcium phosphate coprecipitation method of Searle et al. (*44*). After allowing the cells to recover in DMEM:F12 medium for 5 h, transfected cells were selected by changing the medium and adding fresh culture medium containing 500 μM methotrexate (MTX). After about 10 days of selection in MTX, positive clones were detached from the plates with trypsin and plated in duplicate into 50 mL T-flasks and grown to confluence under MTX selection. For storage, cells were frozen down at this stage in DMEM:F-12, 5% newborn calf serum and 500 μM MTX containing 10% DMSO. For recombinant protein production, the cells were seeded into new T-flasks, and the medium was switched to DMEM:F-12 containing 1% UltraSer G. After 2−3 days, expression levels in the various cell lines were estimated by performing Western blot analysis on samples of the media.

As determined by Western blot analysis, cell lines expressing high levels of recombinant protein were passed sequentially from 50 mL flasks to two 250 mL T-flasks and to expanded surface roller bottles. The cells were allowed to grow to confluence in DMEM:F-12 medium containing 5% NBS and 500 μM MTX; the roller bottles were then switched to DMEM:F-12 medium containing either 0.5% or 1% UltroSer G. The medium was changed every 2−3.5 days. Sodium azide (0.02% w:v) was added to the collected media as an antimicrobial agent, and $Fe(NTA)_2$ was added to saturate the transferrin. The media were pooled and stored at 4 °C until sufficient had been collected to initiate purification. For long-term storage, media were frozen at −20 °C.

Purification of Recombinant Proteins. The tissue culture media were concentrated approximately 10-fold by using a spiral cartridge concentrator. The proteins were purified using the two-step procedure described previously (*45*). The purified protein was lyophilized prior to storage at −20 °C. Protein purity was assessed by UV−vis absorption spectroscopy as well as by polyacrylamide gel electrophoresis in the presence of SDS. Protein concentrations were estimated by using an ELISA using wild-type Tf/2N as a reference. Typical expression levels for the recombinant protein-producing cell lines were in the range 100−200 μg/mL.

All Tf/2N proteins were obtained partially saturated with iron. To obtain the apoproteins, the iron was removed by a literature procedure, in which the iron-protein sample is incubated in a 0.5 M acetate buffer solution at pH 5 containing 1 mM NTA and 1 mM EDTA (*46*). During the preparation of the apoproteins, the mutants showed a qualitative difference in stability. Iron was rapidly removed from Tf/2N, R124A, and R124E, whereas iron removal from K206A and K296A under the same conditions took roughly 20 h. The released Fe(III) and other small molecules such as acetate, NTA, and EDTA, etc., were removed by extensive ultrafiltration in an Amicon cell fitted with a YM 10 membrane.

Spectra of Recombinant hTF/2N. UV−vis spectra of apoproteins and Fe(III) complexes of recombinant and mutant N-lobe half transferrins were recorded on a Hewlett-Packard 8452A Diode Array spectrophotometer equipped with a thermostated cell holder and a circulating water bath at 25.0 °C. A quartz cell with 1 cm path length was used for the routine measurements. The apoproteins were titrated with $Fe(III)(NTA)_2$ to determine extinction coefficients of both apoproteins and their iron complexes.

Kinetics. The iron removal reaction was followed by using visible spectrophotometry to follow changes in the absorbance of the iron(III)-phenolate charge-transfer band near 465 nm. Reactions were carried out in narrow quartz cuvettes (1 mL total volume) with a 1 cm path length. All samples were maintained at 25.0 ± 0.1 °C in 0.10 M Hepes. Pseudo-first-order rate constants were calculated from nonlinear least-squares fits of the absorbance versus time data to the equation

$$A_t = (A_o - A_\infty)e^{-k_{obs}t} + A_\infty \quad (1)$$

where A_t, A_o, and A_∞ are the absorbances at any intermediate time t, time zero, and after infinite time.

The removal of Al^{3+} from transferrin was monitored from changes in the UV spectrum. Equal volumes of an apoTf solution were added to the reference and the sample cuvette, and a baseline of protein vs protein was recorded from 320 to 235 nm. After the addition of 0.8 equiv of Al^{3+} to the sample cuvette and an equal volume of water to the reference cuvette, the value of A_o for the Al−Tf complex was determined for the positive peak in the difference UV spectrum at 240 nm. Following the addition of ligand, the removal of Al^{3+} from the protein was followed by the decrease in the absorbance at 240 nm.

RESULTS

Formation of Iron Complexes. All the apoproteins were titrated with iron to determine the extinction coefficients of both the apoproteins and the ferric−protein complexes. Two well-established methods for the efficient delivery of iron to apoTf at neutral pH are (a) the addition of a ferrous salt, followed by air-oxidation to the ferric−Tf complex, and (b) the addition of the ferric complex of nitrilotriacetic acid (NTA) (*47*). Protein samples were initially titrated with ferric−NTA without any added bicarbonate. We have previously calculated that equilibration with atmospheric CO_2

Table 1: Spectral Characteristics of Fe(III) Complexes of Recombinant Tf/2N and Mutants

protein	λ_{max} (nm)	ϵ_{max} (M^{-1} cm^{-1})	λ_{max} (nm)	ϵ_{max} (M^{-1} cm^{-1})	iron source
Tf/2N	466	2500	278	46500	$Fe(NTA)_2$
R124A	458	2600	280	53500	$FeSO_4$
R124A	472	3300			$Fe(NTA)_2$
R124E	458	1700			$FeSO_4$
K206A	476	2600	280	56500	$Fe(NTA)_2$
K296A	476	2900	278	54500	$Fe(NTA)_2$

will produce an ambient bicarbonate concentration of about 170 μM for a pH 7.4 solution (*48*). The samples contained 50−80 μM protein concentrations, so there was a slight excess of carbonate present for the formation of the usual Fe−CO_3−Tf complexes.

The spectrophotometric titration of Tf/2N with $Fe(NTA)_2$ showed a very clear end point, which was presumed to correspond to the addition of 1 equiv of iron to the protein. The linearity of the titration curve and the sharp end point is consistent with a previous report (*46*) that there is tight binding of Fe^{3+} to the Tf/2N half molecule. The titration curves for K206A and K296A were essentially the same as that for Tf/2N. Extinction coefficients for both the apoproteins and the ferric-protein were calculated assuming that each protein molecule binds one ferric ion. These extinction coefficients are listed in Table 1.

Samples of R124A were titrated with both $Fe(NTA)_2$ and with ferrous ion. Because R124A lacks the arginine residue that is directly involved in binding the synergistic carbonate anion, the protein was titrated with ferrous ion in the presence of 13 mM bicarbonate rather than ambient bicarbonate. There was rapid oxidation and binding of the iron to the protein, and the spectrophotometric titration curve showed a clear endpoint. The resulting iron−R124A complex had a λ_{max} at 458 nm, which is similar to the spectrum of the Fe−CO_3−Tf/2N complex. A λ_{max} of 458 nm has also been reported for the iron complex of the lactoferrin half molecule R121S, in which the corresponding arginine in lactoferrin has been mutated to serine (*49*). The crystal structure of the ferric complex of R121S shows a carbonate anion as a bidentate ligand to the iron (*49*). Thus, the visible spectra indicate that the ferric−R124A complex contains a synergistic carbonate anion.

The presence of carbonate as the synergistic anion in the Fe−CO_3−R124A complex has been confirmed by mass spectroscopy of the Fe−$^{13}CO_3$−R124A complex. The complex was prepared by the addition of ferrous ammonium sulfate in the presence of a large excess of [^{13}C]bicarbonate. The protein solution was dialyzed to remove excess [^{13}C]-bicarbonate from the buffer. An aliquot was then acidified to release the carbonate from the Fe−$^{13}CO_3$−R124A complex as CO_2. The resulting $^{13}CO_2$ was purged from the system, trapped, and injected into a GC-MS. The peak area at mass 45 was used to quantitate the amount of ^{13}C-labeled carbonate in the protein sample. After correcting for background, the ratio of ^{13}C:Fe was 1.0.

A clear spectrophotometric end point is also observed when R124A is titrated with $Fe(NTA)_2$ in the presence of ambient bicarbonate. However, the resulting complex has a λ_{max} at 472 nm, compared with the λ_{max} of 458 observed when the protein was titrated with ferrous ion. The addition of 125 mM bicarbonate to a solution of Fe−R124A prepared from $Fe(NTA)_2$ shifts the λ_{max} from 472 to 458 nm. Thus, it appears that when $Fe(NTA)_2$ is used as the titrant at ambient bicarbonate concentrations, the complex which forms contains NTA as the synergistic anion. Addition of excess bicarbonate shifts the equilibrium in favor of the Fe−CO_3−R124A complex.

The spectra for the Fe−CO_3−R124A and Fe−NTA−R124A complexes have an isosbestic point at 480 nm. This isosbestic point is lost during the conversion of the Fe−NTA−R124A complex to the Fe−CO_3^{2-} -R124A species by the addition of a large excess of $NaHCO_3$. It appears that this reaction does not proceed by simple substitution of CO_3^{2-} for NTA. These results are consistent with an earlier report (*50*) that this anion-exchange reaction actually proceeds in two steps: (1) displacement of Fe(NTA) by the carbonate, and (2) donation of iron from Fe(NTA) to the binary CO_3−protein complex. Very similar results have recently been reported for the reaction of excess bicarbonate with the Fe−NTA−protein complex of the D63S mutant of the N-lobe half-molecule (*19*).

The mutant R124E was also titrated with both $Fe(NTA)_2$ and ferrous ion. In the titration with $Fe(NTA)_2$, there was an increase in the absorbance at 465 nm, but the titration curve lacked a distinct end point. When ferrous ion was used as the titrant, the titration curve did show a clear end point, indicating the formation of a specific 1:1 iron complex whose λ_{max} and extinction coefficient are listed in Table 1. Thus, it appears that R124E can bind iron, but not strongly enough to compete effectively with NTA.

The R124E mutant was prepared with the objective that the carboxylate group of Glu 124 would serve as an endogenous synergistic anion to form a carbonate-free iron−transferrin complex. Unlike the iron complexes of the other mutants, the iron complex of R124E is light yellow. The color of Fe−R124E fades away when the sample is ultrafiltered, even in the presence of 30 mM bicarbonate. This indicates that the Fe−R124E complex is so unstable that it spontaneously dissociates in the absence of chelators when the free iron concentration is decreased by ultrafiltration. It is not clear whether this complex contains carbonate, but since it was too weak to be used in the kinetic studies, the complex has not been investigated further.

Iron Removal from Tf/2N. Rates of iron removal from Tf/2N have been evaluated for the ligands deferiprone, PP_i, and NTA. These ligands have been studied previously with N-terminal monoferric transferrin and show very distinct behavior. Iron removal by deferiprone follows simple saturation kinetics (*21*), iron removal by NTA follows first-order kinetics (*23*), and iron removal by PP_i shows a combination of saturation and first-order components (*27*, *29*, *30*). These ligands were selected to determine how well the Tf/2N half-molecule mimics the range of kinetic behavior that has been observed for iron removal from N-terminal monoferric transferrin.

Iron removal by an excess of the hydroxypyridinone-chelating agent deferiprone follows first-order kinetics with respect to the concentration of Fe-Tf/2N. The apparent first-order rate constant for this reaction has been measured as a function of the ligand concentration. A plot of k_{obs} versus [deferiprone] is shown in Figure 1. Iron removal follows simple saturation kinetics with respect to the ligand concen-

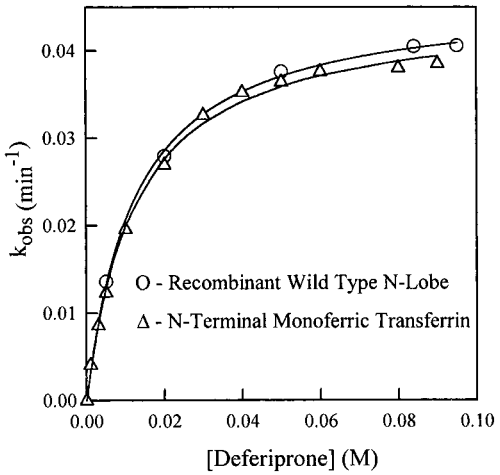

FIGURE 1: Dependence of observed rate constants for the removal of iron from Tf/2N (○) and from Tf-Fe_N (△) on the concentration of deferiprone in 0.10 M Hepes, pH 7.4 at 25 °C. The solid lines represent least-squares fits of the data to eq 2.

Table 2: Kinetic Parameters for Iron Removal from the N-Lobe of Transferrin

	k_{max} (min^{-1})	k_d (mM)	k'''(min^{-1} M^{-1})
Tf/2N			
deferiprone	0.046 ± 0.001	12.5 ± 0.7	
NTA			0.22 ± 0.02
PP_i	0.036 ± 0.004	2.6 ± 0.9	0.90 ± 0.06
R124A			
deferiprone			980 ± 60
AHA			56.7 ± 0.6
Tf-Fe_N			
deferiprone[a]	0.045	12.5	
NTA[b]			0.21
PP_ic	0.051	16.9	0.25

[a] Data from ref *21*. [b] Data from ref *23*. [c] Data from ref *27*.

Table 3: Kinetics Parameters for Al^{3+} Removal from Transferrin Half Molecules by PP_i

	k_{max} (min^{-1})	k_d (mM)	k''' (min^{-1} M^{-1})
Tf/2N	0.31 ± 0.02	0.061 ± 0.001	311 ± 15
K296A	0.0092 ± 0.0002	31.0 ± 0.2	
K206A	0.0122 ± 0.0003	14.5 ± 0.2	

tration. The results can be described by the empirical equation

$$k_{obs} = \frac{k_{max}[L]}{k_d + [L]} \quad (2)$$

The observed rate parameters for Tf/2N are $k_{max} = 0.046 \pm 0.001$ min^{-1} and $k_d = 12.5 \pm 0.7$ mM. For comparison, data for iron removal from N-terminal monoferric transferrin from Li and Harris (*21*) are also shown in Figure 1. It is clear that N-terminal monoferric Tf and Fe-Tf/2N show essentially identical kinetic behavior for iron removal by deferiprone. The kinetic parameters for iron removal from both Tf-Fe_N and Tf/2N are listed in Table 2.

Kinetic data for iron removal from Fe-Tf/2N by NTA are shown in Figure 2, along with previous results for iron removal from N-terminal monoferric transferrin (*23*). Once again, the data for the Tf/2N half molecule are essentially identical to those for N-terminal monoferric transferrin. Both systems show simple first-order kinetics with respect to the

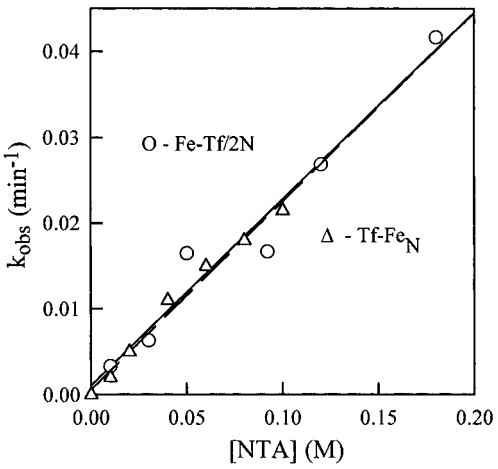

FIGURE 2: Dependence of observed rate constants for the removal of iron from Tf/2N (○) and from Tf-Fe_N (△) on the concentration of NTA in 0.10 M Hepes, pH 7.4 at 25 °C. The solid and dashed lines are linear least-squares fits of the data.

ligand, with rate constants of 0.218 ± 0.023 min^{-1} M^{-1} for Fe-Tf/2N and 0.212 min^{-1} M^{-1} for Tf-Fe_N. The data for Tf/2N extend to higher NTA concentrations, 180 mM, but there is still no sign of curvature in the plot. In addition, the intercept is only 0.001 ± 0.002, so there is no evidence of a saturation component for iron removal by NTA.

The results for iron removal from Fe-Tf/2N by PP_i are shown in Figure 3. Iron removal by this ligand shows a more complex ligand dependence. Instead of reaching a plateau, k_{obs} continues to increase at higher ligand concentrations. A calculated fit of the pyrophosphate data to eq 2 was very poor. As shown in several previous studies (*18*, *23*, *24*, *27*, *28*), data of this type can be fit very well by adding a first-order term to eq 2 to obtain

$$k_{obs} = \frac{k_{max}[L]}{k_d + [L]} + k'''[L] \quad (3)$$

A fit of the PP_i data to eq 3, shown by the solid line in Figure 3, results in the fitting parameters listed in Table 2.

The dashed line in Figure 3 shows the calculated curve for iron removal from Tf-Fe_N based on the kinetics parameters previously reported by Bali and Harris (*27*). Unlike the reactions with deferiprone and NTA, there appears to be a significant discrepancy between the rate of iron removal from Tf/2N and from Tf-Fe_N. Iron removal from these two proteins by 100 mM PP_i has also been measured by Zak et al. (*51*), and their results are shown as the triangles in Figure 3. There is excellent agreement between the two studies on the Tf-Fe_N system, while we report a slightly higher rate constant for iron removal from Tf/2N. In both studies, there is a significant difference between the rate constants for Tf/2N and Tf-Fe_N.

Iron removal from Fe-Tf/2N by PP_i was also evaluated for solutions that contained 400 mM Cl^- (as NaCl). The addition of the Cl^- anion results in a significant reduction in the rate of iron removal. The data appear to follow first-order kinetics, but with a nonzero *y*-intercept. We infer that the nonzero intercept is due to a saturation component, but since it is not possible to detect any curvature at the beginning of the plot, it appears that $[L] \gg k_d$ even at the lowest concentration of PP_i. Thus, the data can be fit to the

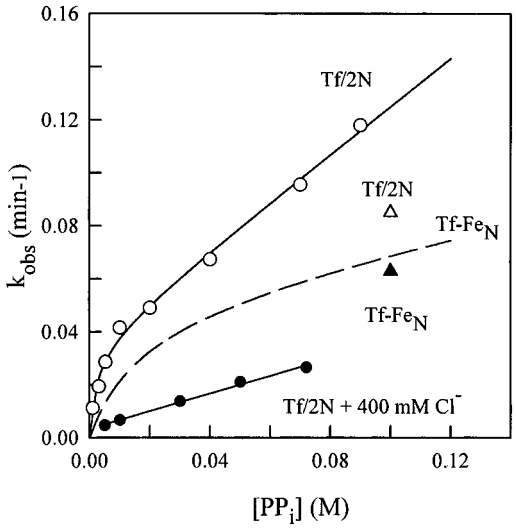

FIGURE 3: Dependence of observed rate constants for iron removal from Tf/2N on the concentration of PP_i in 0.10 M Hepes, pH 7.4, at 25 °C, in the absence of Cl^- (○) and in the presence of 0.4 M Cl^- (●). The solid line represents a least-squares fit of the data to eq 3. The dashed line is the calculated curve for Tf-Fe_N based on the kinetic parameters reported by Bali and Harris (*27*). The triangles represent the rate constants measured by Zak et al. (*51*) for iron removal by 100 mM PP_i from Tf/2N (△) and from Tf-Fe_N (▲).

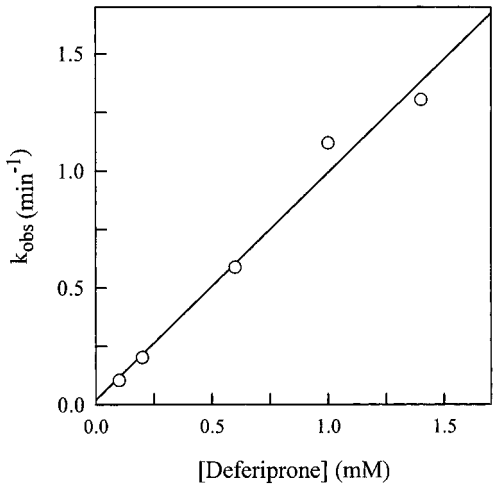

FIGURE 4: Dependence of observed rate constants for iron removal from R124A-Fe(III) on the concentration of deferiprone in 0.10 M Hepes, pH 7.4, at 25 °C. The solid line is a linear least-squares fit of the data.

equation

$$k_{obs} = k_{max} + k'''[L] \quad (4)$$

to calculate values of $k_{max} = 0.0035 \pm 0.0006$ min^{-1} and $k''' = 0.332 \pm 0.015$ min^{-1} M^{-1}. The presence of chloride reduces k_{max} to about 10% of its original value and k''' to about 35% of its original value.

Iron Removal from Mutant N-Lobe Proteins. The ligand dependence for the removal of iron from R124A by deferiprone is shown in Figure 4. The most striking observation is that the ligand dependence for R124A has changed from the simple saturation kinetics with respect to ligand observed for Tf/2N to simple first order kinetics, with a relatively large rate constant of 980 ± 60 min^{-1} M^{-1}. At a concentration of 100 mM deferiprone, iron removal from R124A is about 2500 times faster than iron removal from Tf/2N.

Very similar results were observed for iron removal from R12A by AHA. This reaction also switched from saturation kinetics to first-order kinetics with respect to the concentration of AHA. The reaction is not as rapid with AHA as it is with deferiprone. The rate constant for AHA is only 56.7 ± 0.6 min^{-1}. Nevertheless, at 100 mM AHA, iron removal from R124A is still about 300 times faster than iron removal from Fe-Tf/2N (*21*).

When we attempted to study iron removal from K206A and K296A with ~80 mM concentrations of NTA and deferiprone, it appeared that essentially no iron was removed over a 4 h period. Even the use of more powerful iron-chelating agents, 100 mM *N*,*N*′-di(5-sulfo-2-hydroxybenzyl)-ethylenediamine-*N*,*N*′-diacetic acid and 180 mM ethylenediaminetetra(aminomethyl)phosphonic acid, failed to produce any detectable iron release after 4 h. We were able to observe a small absorbance change from 0.30 to ~0.26 by increasing the concentration of Fe(III)−K206A from 20 to 110 μM and following the reaction with 0.1 M PP_i for more than 60 h. From these data, we can only estimate a rate constant of about 1×10^{-5} min^{-1}. Because of the slow rate of release and/or thermodynamic stability of the ferric complexes with K206A and K296A, no detailed kinetic studies were possible.

Kinetic Studies on Al^{3+}-Tf/2N. Because the rates of iron removal from the lysine mutants K206A and K296A were so slow, kinetic studies were conducted using the more labile Al^{3+} ion as a model for Fe^{3+}. To confirm that the recombinant N-lobe proteins bind Al^{3+}, protein samples were first titrated with Al^{3+} and the binding was monitored by difference UV spectroscopy. Binding of Al^{3+} to Tf/2N, K296A, and K206A produces the characteristic peak for metal binding near 245 nm in the difference UV spectrum. Titration of each protein with an acidic solution of $AlCl_3$ results in a linear absorbance increase until the end point is reached at 1 equiv of Al. The lack of curvature indicates relatively strong binding of the Al. The kinetics of metal binding are much slower for both K296A and K206A. About 1 h was required to reach equilibrium following each addition of Al.

First-order rate constants for the removal of Al^{3+} from Tf/2N were measured for a series of PP_i concentrations, and the results are plotted in Figure 5. This system shows the same combination of saturation and first-order kinetics that were observed for iron removal by PP_i. However, the rate constants for Al^{3+} are significantly larger, with $k_{max} = 0.31 \pm 0.02$ min^{-1} for Al^{3+} compared with 0.036 min^{-1} for iron and $k''' = 311 \pm 15$ min^{-1}M^{-1} for Al^{3+} compared with 0.9 min^{-1}M^{-1} for Fe^{3+}. Furthermore, the saturation component of the aluminum reaction reaches saturation at a much lower ligand concentration, with $k_d = 0.061 \pm 0.001$ mM for Al^{3+} vs 2.6 mM for Fe^{3+}.

Similar kinetic studies were also carried out using the Al^{3+} complexes of both K206A and K296A, and the resulting ligand dependence curves are plotted in Figure 6. There are very significant differences between Tf/2N and the two lysine mutants. First, the value of k_{max} drops dramatically, from 0.31 min^{-1} for Tf/2N to only 0.0122 min^{-1} for K296A and 0.0092 min^{-1} for K206A. In addition, the k_d values increase substantially for the mutants (31 mM for K206A and 14.5 mM for K296A), so that much higher concentrations of PP_i are required to reach saturation. Last, the first-order

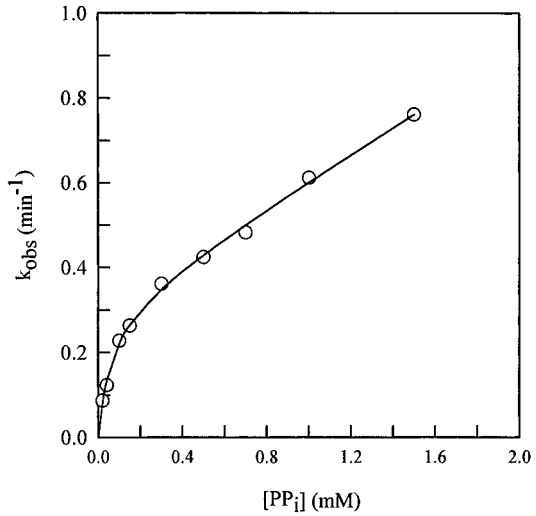

FIGURE 5: Dependence of the rate constant for Al^{3+} removal from Tf/2N on the concentration of PP_i in 0.1 M Hepes, pH 7.4, at 25 °C. The solid line represents a least-squares fit of the data to eq 3.

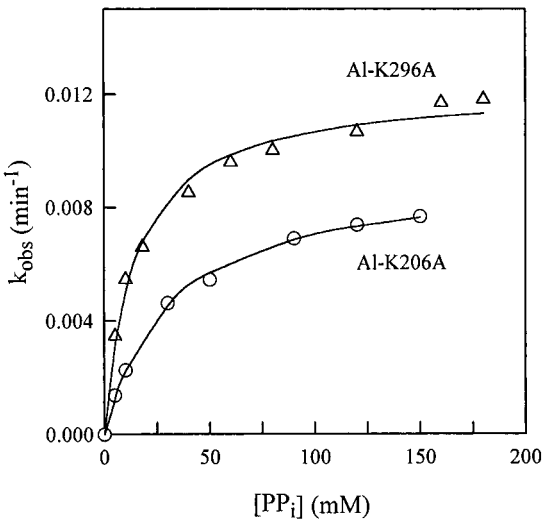

FIGURE 6: Dependence of the rate constants for the removal of Al^{3+} from K206A (○) and from K296A (△) on the concentration of PP_i in 0.10 M Hepes, pH 7.4, at 25 °C. The solid lines represent fits of the data to eq 2.

component for Al removal, which is very significant for Tf/2N, is essentially eliminated in both K206A and K296A. All these factors work together to produce a very dramatic reduction in the overall rate of Al removal from the lysine mutants.

Lysine 206 and 296 are near the metal-binding site, but do not directly interact with the bound metal ion. It has been suggested that they may be involved in an allosteric anion-binding site, i.e., the KISAB site (*4*, *5*, *37*, *38*). If so, one might expect that the rate of metal removal from K206A and K296A might lack the usual sensitivity to inorganic anions. The rate of Al^{3+} removal from both proteins by PP_i was evaluated as a function of the concentration of $NaClO_4$, and the results are plotted in Figure 7. Contrary to our expectations, both proteins show the same decrease in rate constant with increasing [ClO_4^-] that has been repeatedly observed for the removal of iron from the N-terminal site by several ligands (*18*, *30*, *31*, *34*, *35*). This suggests that the Lys 296−Lys 206 pair is not a critical component of the KISAB site.

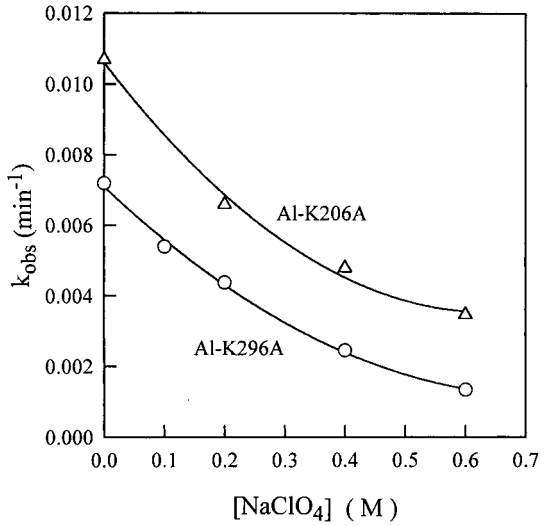

FIGURE 7: Observed rate constants for the removal of Al^{3+} from K296A (○) and from K206A (△) by 120 mM PP_i as a function of the $NaClO_4$ concentration in 0.1 M Hepes, pH 7.4, at 25 °C.

DISCUSSION

For iron removal by deferiprone and NTA, there is exceptionally good agreement between the kinetic data on the Tf/2N half-molecule and N-terminal monoferric transferrin. There is also very good agreement between studies on iron removal by tiron from diferric transferrin and Tf/2N. Iron removal from diferric transferrin is biphasic, with both the larger and smaller rate constants showing simple saturation kinetics with respect to the tiron concentration (*22*). Iron removal from Tf/2N by tiron also follows simple saturation kinetics (*19*), and the k_{max} for Tf/2N agrees quite well with the faster of the two rate constants for iron removal from diferric transferrin. These results indicate that the N-terminal half-molecule is an excellent model for both the saturation and first-order components of iron removal from the N-terminal lobe of the holoprotein. This relative independence of the two transferrin lobes is consistent with studies on cobalt-labeled monoferric transferrins, which have tended to show that binding cobalt(III) at one site has relatively little effect on iron release from the other site (*18*, *23*, *24*, *27*).

The results with PP_i appear to contradict this generalization, as there is a clear difference in the behavior of Tf/2N vs Tf-Fe_N. In our previous study on iron removal from Fe-Tf_N by PP_i, we prepared the stock PP_i solutions from the tetrasodium salt. To adjust the stock solution to pH 7.4, it was necessary to add about 1 equiv of acid, and in that study, HCl was used. Thus, each kinetic sample contained approximately equimolar Cl^- and PP_i, and the concentration of Cl^- varied as the ligand concentration varied. Considering that the present study indicates that Cl^- retards iron release from Tf/2N, the presence of Cl^- in the PP_i solutions could be at least partly responsible for the slower rate of iron release reported for Tf-Fe_N compared to the new results reported here on Tf/2N. Similarly, the slightly low rate constant reported by Zak et al. (*51*) for iron removal from Tf/2N could be due in part to the presence of 100 mM Cl^- ion in their sample.

A more definitive analysis of the results with PP_i is hampered by the variation in the Cl^- concentration among

different studies and discrepancies among the reported effects of Cl^- on the rate of iron removal by PP_i. A previous study from this laboratory failed to detect a significant effect of the Cl^- ion on the rate of iron removal from Tf-Fe_N (*35*), and Zak et al. (*51*) observed almost no difference in the rate of iron removal from Tf/2N between solutions containing 100 and 600 mM Cl^-. Marques et al. (*30*) reported that Cl^- caused a very slight retardation of iron removal by 5 mM PP_i, but caused a substantial acceleration in the rate of iron removal by 100 mM PP_i. With respect to iron removal from Tf/2N by other ligands, chloride causes a modest decrease in the rate of iron release from tiron (*19*) and a much more significant decrease for iron removal by EDTA (*52*). In addition, the effect of Cl^- on iron removal from Tf/2N appears to be pH dependent (*19*, *52*). Thus, additional studies under more carefully controlled conditions will be required to determine the extent to which iron removal by PP_i varies between Tf/2N and Tf-Fe_N.

In our previous evaluation of iron removal by PP_i from N-terminal monoferric transferrin, we reported that there was relatively little difference between the quality of the two- and three-parameter fits to eqs 2 and 3 (*27*). Since that paper appeared, it has become increasingly clear that the results from the three-parameter fit to eq 3 are more consistent with data on other phosphonate ligands. In addition, Marques et al. (*30*) have reported a combination of saturation and first-order kinetics for PP_i that is consistent only with eq 3. The present study on Tf/2N further supports the conclusion that iron removal from the N-terminal site is best described as a combination of saturation and first-order components.

Even though both Al^{3+} and Fe^{3+} complexes of Tf/2N show the same combination of saturation and first-order components, the k_{max} for the Al-Tf/2N complex is obviously much larger. Citrate also removes aluminum much more quickly than iron (*53*). The relatively slow rates of metal release and the large variation in reaction rates between the aluminum and iron complexes suggest that the rate-limiting conformational change in the protein may involve the breaking of at least one metal−ligand bond. Asp 63 is the only ligand originating from domain I of the N-lobe, and others have suggested that it is the binding of this ligand that closes the interdomain cleft (*38*, *54*). Thus, it seems likely that breaking of the metal−aspartate bond would be an early and perhaps rate-limiting step in iron release.

EDTA has been used to study the iron removal kinetics of both Tf-Fe_N (*18*) and D63S (*52*). Removal of the aspartate ligand increases the rate of iron removal by more than 2 orders of magnitude. On the basis of the solution X-ray-scattering results, which indicate that there is little conformation change in the D63S mutant when the iron binds (*54*), it is tempting to attribute the faster rate of iron release from the D63 mutants to a more widely open interdomain cleft. However, the X-ray structure of the corresponding lactoferrin mutant D60S shows that the interdomain cleft is actually more closed, rather than more open (*55*). The kinetic results are more consistent with the hypothesis that the rate-determining step in iron removal involves breaking the iron−aspartate bond. The D63S mutant continues to show saturation kinetics with respect to the concentration of EDTA. Once the metal−aspartate bond has been broken, the rate of iron release may be regulated by other, more rapid, conformational changes along a reaction pathway to the fully open form of the apoprotein.

Iron Removal from R124 Mutants. Even though Arg 124 has often been described as the "essential" arginine because of its role in binding the synergistic carbonate anion, it is now clear that although mutations of this residue weaken iron binding, the arginine side chain is not essential for iron binding. Zak et al. (*51*) have shown that both R124S and R124K still bind iron. This study extends the series of Arg 124 mutants to include substitution by alanine, which has no coordinating or hydrogen-bonding capabilities. The ^{13}C mass spectrometry results reported here confirm that CO_3^{2-} is acting as the synergistic anion in the Fe^{3+} complex with R124A.

Faber et al. (*49*) have mutated the corresponding arginine residue in the N-lobe of lactoferrin to give the R121E and R121S mutants. Although these proteins form relatively weak ferric complexes, crystal structures were obtained showing that both complexes contain carbonate in its usual position as a bidentate ligating group on the iron even though there are no stabilizing interactions between the carbonate and the serine or glutamate side chains. The mutations cause little change in the first-coordination sphere of the ferric ion, but they do shift the carbonate about 0.5 Å in such a way as to weaken the hydrogen-bonding interaction between the carbonate and the N-terminus of helix 5. Given this and the loss of the hydrogen bonds to arginine, one would clearly expect that the carbonate would be bound more loosely in the arginine mutants than in Tf/2N.

Iron release by deferiprone and AHA from R124A is much faster than iron release from Tf/2N. In addition, the order of the reaction changes, from simple saturation kinetics for iron removal from Tf/2N to simple first-order kinetics from R124A. Thus, the conformational gating associated with the transferrins disappears in the R124A mutant. Since the lactoferrin structures for R121S and R121E do not show major structural changes, we are reluctant to conclude that the interdomain cleft is much more open in the ferric complex of R124A. Instead, it appears that a more weakly bound carbonate anion allows for the very efficient displacement of the carbonate anion by the ligand in a first-order process for iron removal.

These results are consistent with our previous suggestion that there is a separate first-order pathway for iron removal that involves the substitution of the synergistic carbonate by an anionic moiety from the incoming ligand (*18*, *23*, *24*). This proposal was based in large part on the observations that iron removal from N-terminal monoferric transferrin by NTA followed simple first-order kinetics (*23*), and that NTA is an effective substitute for the synergistic carbonate anion (*56*). These new results on iron removal from Fe-Tf/2N confirm that the reaction is simple first-order with respect to the concentration of NTA. In addition, the concentration range of NTA that was used is even wider than in the previous study, with no indication of curvature in the plot.

Bailey et al. (*26*) have measured the rates of iron release by PP_i from ovotransferrin that has been chemically modified to include an endogenous carboxylate group that serves in place of carbonate as the synergistic anion. One assumes that the endogenous ligand will be more difficult to displace, and indeed the first-order component that one normally observes for iron release by PP_i is lost with the

modified protein. These observations also support the hypothesis that the first-order kinetic component is tied to the ability of the incoming ligand to displace the synergistic carbonate anion. This reaction appears to depend in a very complex way on the structure of the protein, the strength of the protein−carbonate interactions, and the structure of the incoming ligand.

It has also been suggested that the first-order component might result from the binding of charged ligands to the allosteric KISAB site associated with the effect of inorganic salts on the rates of iron removal (*28*−*30*, *37*). We have recently shown that a first-order component for iron removal could be generated simply by using the hydrochloride salt of deferiprone instead of the free base (*21*), so clearly one must be concerned about the allosteric effects from binding anionic ligands to the KISAB site. It may well be that allosteric binding of ligands is responsible for some of the variations in k_{max} observed for different ligands (*21*) and for the appearance of minor first-order kinetic terms. However, we do not feel that results such as those for NTA, where the first-order term is in fact the only component of iron removal, can be reasonably interpreted as allosteric perturbations of a simple saturation, conformational gating mechanism.

Metal Release from K206A and K296A. The residues Lys 206 and Lys 296 are suspected of playing an important role in the binding and release of iron. Dewan et al. (*9*) have pointed out that these residues, which are conserved in the N-lobes of most transferrins, form a very short hydrogen bond in the closed conformation of the iron−protein complexes. It has been proposed that protonation of both lysines could be a critical component in the release of iron at lower pH (*4*, *9*, *12*, *37*, *51*), and there has been speculation that these residues may play a significant role in the effects of anions on the kinetics of iron removal (*4*, *5*, *37*).

Both K206Q (*46*) and K206R (*51*) appear to form very stable iron−protein complexes. Zak et al. (*51*) have shown that iron removal by PP_i from K206R, in which the cationic lysine side chain is replaced by another cationic side chain, proceeds at about two-thirds of the rate of iron release from Tf/2N. We now report a much more dramatic decrease in the rate of iron removal from both K206A and K296A, in which a lysine residue is replaced by a neutral alanine side chain. The rates of iron removal at pH 7.4 are essentially too slow to study.

To give reactions that proceed within a reasonable time period, kinetic studies have been conducted on the Al^{3+} complexes of Tf/2N, K206A, and K296A. The studies on Tf/2N show that Al^{3+} removal by PP_i includes both saturation and first-order components, just as observed for iron removal. Thus, Al^{3+} appears to be a good functional model for Fe^{3+} in terms of iron release kinetics. Figure 6 shows that the kinetics convert to simple saturation kinetics for both K206A and K296A and that the k_{max} for the saturation component drops from about 0.31 min^{-1} for Tf/2N to about 0.01 min^{-1} for the lysine mutants. If k_{max} is associated with a rate-limiting protein conformational change, then it appears that eliminating the K206−K296 interaction reduces the rate of this conformational change by about a factor of 30.

At higher concentrations of PP_i, the disparity in the rates of Al removal between Tf/2N and the lysine mutants grows even larger due to the lack of a first-order component in the lysine mutants. At 100 mM PP_i, aluminum removal from Tf/2N is approximately 3000 times faster than removal from the lysine mutants. If this same ratio applies to the rates of iron removal, then one can use the rate constant for iron removal from Tf/2N to estimate a rate constant for the removal of iron from the lysine mutants of about 4×10^{-5} min^{-1}. This is close to the value of 1×10^{-5} min^{-1} that we had estimated based on the very limited data on iron removal from the lysine mutants. This is another indication that the aluminum(III)−protein complexes are excellent models for the kinetic behavior of the corresponding iron complexes.

Figure 7 shows that the retarding effect of perchlorate on metal ion removal is retained for both K206A and K296A. Although these residues are clearly important in regulating the conformational change that controls k_{max}, it appears that these lysines are not a critical component of the anion-sensitive KISAB site. Even though the KISAB site still appears to be functional in K206A and K292A, the first-order component for Al^{3+} removal is lost in both mutants. This provides further evidence against the hypothesis that the first-order component for metal removal by PP_i is tied to the binding of the ligand to the KISAB site. It is interesting that Grady et al. (*57*) can detect Cl^- binding to the ferric complexes of both K206Q and K296Q from changes in the EPR spectrum. Whether the EPR experiments are detecting binding at the KISAB remains to be seen.

REFERENCES

1. Brock, J. H. (1985) in *Metalloproteins, Part II* (Harrison, P., Ed.) pp 183−262, Macmillan, London.
2. Baker, E. N. (1993) in *Perspectives on Bioinorganic Chemistry* (Hay, R. W., Dilworth, J. R., and Nolan, K. B., Eds.) pp 161−205, JAI Press, London.
3. Aisen, P. (1989) in *Iron Carriers and Iron Proteins* (Loehr, T. M., Ed.) pp 353−371, VCH, New York.
4. Baker, E. N., and Lindley, P. F. (1992) *J. Inorg. Biochem. 47*, 147−160.
5. Baker, E. N. (1994) *Adv. Inorg. Chem. 41*, 389−463.
6. Anderson, B. F., Baker, H. M., Norris, G. E., Rumball, S. V., and Baker, E. N. (1990) *Nature 344*, 784−787.
7. Bailey, S., Evans, R. W., Garratt, R. C., Gorinsky, B., Hasnain, S., Horsburgh, C., Jhoti, H., Lindley, P. F., Mydin, A., Sarra, R., and Watson, J. L. (1988) *Biochemistry 27*, 5804−5812.
8. Sarra, R., Garratt, R., Gorinsky, B., Jhoti, H., and Lindley, P. (1990) *Acta Crystallogr., Sect. B 46*, 763−771.
9. Dewan, J. C., Mikami, B., Hirose, M., and Sacchettini, J. C. (1993) *Biochemistry 32*, 11963−11968.
10. Haridas, M., Anderson, B. F., and Baker, E. N. (1995) *Acta Crystallogr., Sect. D 51*, 629−646.
11. Day, C. L., Anderson, B. F., Tweedie, J. W., and Baker, E. N. (1993) *J. Mol. Biol. 232*, 1084−1100.
12. Kurokawa, H., Mikami, B., and Hirose, M. (1995) *J. Mol. Biol. 254*, 196−207.
13. Rawas, A., Muirhead, H., and Williams, J. (1996) *Acta Crystallogr., Sect. D 52*, 631−640.
14. Moore, S. A., Anderson, B. F., Groom, C. R., Haridas, M., and Baker, E. N. (1997) *J. Mol. Biol. 274*, 222−236.
15. Rawas, A., Muirhead, H., and Williams, J. (1997) *Acta Crystallogr., Sect. D 53*, 464−468.
16. MacGillivray, R. T. A., Moore, S. A., Chen, J., Anderson, B. F., Baker, H., Luo, Y., Bewley, M., Smith, C. A., Murphy, M. E. P., Wang, Y., Mason, A. B., Woodworth, R. C., Brayer, G. D., and Baker, E. N. (1998) *Biochemistry 37*, 7919−7928.
17. Cowart, R. E., Kojima, N., and Bates, G. W. (1982) *J. Biol. Chem. 257*, 7560−7565.
18. Harris, W. R., and Bao, G. (1997) *Polyhedron 16*, 1069−1079.
19. He, Q.-Y., Mason, A. B., Woodworth, R. C., Tam, B. M., Wadsworth, T., and MacGillivray, R. T. A. (1997) *Biochemistry 36*, 5522−5528.

20. Kretchmar, S. A., and Raymond, K. N. (1986) *J. Am. Chem. Soc. 108*, 6212−6218.
21. Li, Y., and Harris, W. R. (1998) *Biochim. Biophys. Acta* (in press).
22. Kretchmar Nguyen, S. A., Craig, A., and Raymond, K. N. (1993) *J. Am. Chem. Soc. 115*, 6758−6764.
23. Bali, P. K., Harris, W. R., and Nesset-Tollefson, D. (1991) *Inorg. Chem. 30*, 502−508.
24. Harris, W. R., Bali, P. K., and Crowley, M. M. (1992) *Inorg. Chem. 31*, 2700−2705.
25. Marques, H. M., Watson, D. L., and Egan, T. J. (1991) *Inorg. Chem. 30*, 3758−3762.
26. Bailey, C. T., Byrne, C., Chrispell, K., Molkenbur, C., Sackett, M., Reid, K., McCollum, K., Vibbard, D., and Catelli, R. (1997) *Biochemistry 36*, 10105−10108.
27. Bali, P. K., and Harris, W. R. (1989) *J. Am. Chem. Soc. 111*, 4457−4461.
28. Bertini, I., Hirose, J., Luchinat, C., Messori, L., Piccioli, M., and Scozzafava, A. (1988) *Inorg. Chem. 27*, 2405−2409.
29. Egan, T. J., Ross, D. C., Purves, L. R., and Adams, P. A. (1992) *Inorg. Chem. 31*, 1994−1998.
30. Marques, H. M., Egan, T. J., and Pattrick, G. (1990) *S. Afr. J. Sci. 86*, 21−24.
31. Baldwin, D. A., and de Sousa, D. M. R. (1981) *Biochem. Biophys. Res. Commun. 99*, 1101−1107.
32. Egan, T. J., Zak, O., and Aisen, P. (1993) *Biochemistry 32*, 8162−8167.
33. Kretchmar, S. A., and Raymond, K. N. (1988) *Inorg. Chem. 27*, 1436−1441.
34. Thompson, C. P., McCarty, B. M., and Chasteen, N. D. (1986) *Biochim. Biophys. Acta 870*, 530−537.
35. Harris, W. R., and Bali, P. K. (1988) *Inorg. Chem. 27*, 2687−2691.
36. Baldwin, D. A. (1980) *Biochim. Biophys. Acta 623*, 183−198.
37. Egan, T. J., Ross, D. C., and Purves, L. R. (1994) *S. Afr. J. Sci. 90*, 539−543.
38. Lindley, P. F., Bajaj, M., Evans, R. W., Garratt, R. C., Hasnain, S. S., Jhoti, H., Kuser, P., Neu, M., Patel, K., Sarra, R., Strange, R., and Walton, A. (1993) *Acta Crystallogr., Sect. D 49*, 292−304.
39. Gale, G. R., Litchenberg, W. H., Smith, A. B., Singh, P. K., Campbell, R. A., and Jones, M. M. (1991) *Res. Commun. Chem. Pathol. Pharmacol. 73*, 299−313.
40. Funk, W. D., MacGillivray, R. T. A., Mason, A. B., Brown, S. A., and Woodworth, R. C. (1990) *Biochemistry 29*, 1654−1660.
41. Palmiter, R. D., Behringer, R. R., Quaife, C. J., Maxwell, F., Maxwell, I. H., and Brinster, R. L. (1987) *Cell 50*, 435−443.
42. Nelson, R. M., and Long, G. L. (1989) *Anal. Biochem. 180*, 147−151.
43. Yang, F., Lum, J. B., McGill, J. R., Moore, C. M., Naylor, S. L., Van Bragt, P. H., Baldwin, W. D., and Bowman, B. H. (1984) *Proc. Natl. Acad. Sci. U.S.A. 81*, 2752−2756.
44. Searle, P. F., Stuart, G. W., and Palmiter, R. D. (1985) *Mol. Cell. Biol. 5*, 1480−1489.
45. Mason, A. B., Funk, W. D., MacGillivray, R. T. A., and Woodworth, R. C. (1991) *Protein Expression Purif. 2*, 214−220.
46. Woodworth, R. C., Mason, A. B., Funk, W. D., and MacGillivray, R. T. A. (1991) *Biochemistry 30*, 10824−10829.
47. Chasteen, N. D. (1977) *Coord. Chem. Rev. 22*, 1−36.
48. Harris, W. R., and Stenback, J. Z. (1988) *J. Inorg. Biochem. 33*, 211−223.
49. Faber, H. R., Baker, C. J., Day, C. L., Tweedie, J. W., and Baker, E. N. (1996) *Biochemistry 35*, 14473−14479.
50. Rogers, T. B., Feeney, R., and Meares, C. F. (1977) *J. Biol. Chem. 252*, 8108−8112.
51. Zak, O., Aisen, P., Crawley, J. B., Joannou, C. L., Patel, K. J., Rafiq, M., and Evans, R. W. (1995) *Biochemistry 34*, 14428−14434.
52. He, Q.-Y., Mason, A. B., and Woodworth, R. C. (1997) *Biochem. J. 328*, 439−445.
53. Marques, H. M. (1991) *J. Inorg. Biochem. 41*, 187−193.
54. Grossmann, J. G., Mason, A. B., Woodworth, R. C., Neu, M., Lindley, P. F., and Hasnain, S. S. (1993) *J. Mol. Biol. 231*, 554−558.
55. Faber, H. R., Bland, T., Day, C. L., Norris, G. E., Tweedie, J. W., and Baker, E. N. (1996) *J. Mol. Biol. 256*, 352−363.
56. Schlabach, M. R., and Bates, G. W. (1975) *J. Biol. Chem. 250*, 2182−2188.
57. Grady, J. K., Mason, A. B., Woodworth, R. C., and Chasteen, N. D. (1995) *Biochem. J. 309*, 403−410.

BI9810454